Available online at www.sciencedirect.com
ScienceDirect
Journal of Magnetic Resonance 189 (2007) 151–155
JMR Journal of Magnetic Resonance
www.elsevier.com/locate/jmr

Communication

Absolute quantification of Na^+ bound fraction by double-quantum filtered ^{23}Na NMR spectroscopy

Mohamed Mouaddab, Loïc Foucat *, Jean Pierre Donnat, Jean Pierre Renou, Jean Marie Bonny

Structures Tissulaires et Interactions Moléculaires, UR370, INRA-Theix, 63122 Saint-Genes-Champanelle, France

Received 26 July 2007; revised 5 September 2007
Available online 11 September 2007

Abstract

A method is described for the absolute quantification of double-quantum filtered spectra of spin-3/2 nuclei (^{23}Na). The method was tested on a model system, a cationic exchange resin for which the number of Na^+ binding sites was quantitatively controlled. The theoretical and experimental approaches were validated on samples with different Na^+ concentrations. An excellent agreement between the results obtained by double-quantum and single-quantum acquisitions was found. This method paves the way for absolute quantification of both bound and free fractions of Na^+, which are determining factors in the characterization of salted/brined/dried food products.

Keywords: Sodium NMR; Double-quantum-filter; Absolute quantification; Cationic exchange resin

1. Introduction

NMR measurements on spin-3/2 quadrupolar sodium nuclei (^{23}Na) are widely used to investigate structure and dynamics in material science, e.g., in porous materials [1,2], in biopolymers [3], biological tissue such as cartilage, skeletal muscle and brain [4,5] and in living plants [6], and more recently in food science [7–10]. In this last field, it is well known that sodium chloride is one of the most widely used ingredients in food processing. It affects the sensory and technological properties of food products, e.g., flavor, texture and shelf life. In particular, because sodium intake exceeds nutritional recommendations in many industrialized countries, reducing salt content is currently a challenge for the food industry [11]. There is thus a need to characterize and quantify the state and content of sodium ions in such products.

For this purpose, ^{23}Na NMR offers a unique means to assess the content and binding state of Na^+ ions non-invasively. ^{23}Na multiple-quantum-filtered (MQF) NMR has been shown to be useful for selectively detecting sodium ions experiencing anisotropic motion due to their interactions with ordered structures [12]. However, only a few studies have focused on the absolute quantification of Na^+ concentration [13–15].

The objective of this study was to demonstrate that double-quantum-filtered (DQF) ^{23}Na NMR spectroscopy could be used to determine bound Na^+ concentration precisely. To this end, a quantitative experimental design was developed, based on double-quantum and single-quantum (DQ and SQ) experiments, with appropriate data analysis. To test and validate the method, an ion exchange resin was chosen as a model. This original system makes it possible to define and control the nature and number of sodium ion binding sites.

2. Theoretical background

The dominant relaxation mechanism of spin-3/2 nuclei is the fluctuating quadrupolar interaction between the nuclear electric quadrupole moment and the local electrostatic field

* Corresponding author. Fax: +33 4 73 62 41 89.
E-mail address: lf@clermont.inra.fr (L. Foucat).

1090-7807/$ - see front matter © 2007 Elsevier Inc. All rights reserved.
doi:10.1016/j.jmr.2007.09.003

gradient [3,16]. Biexponential relaxation is observed when the extreme narrowing condition does not hold [17]. Under such conditions the outer transitions ($-3/2 \rightarrow -1/2$ and $1/2 \rightarrow 3/2$) decay more quickly than the inner transition ($-1/2 \rightarrow 1/2$). The transverse relaxation times T_{2F} and T_{2S} characterize these "Fast" and "Slow" decays, respectively. Biexponential relaxation induces violations of coherence transfer selection rules that can be described by representing the evolution of coherence in terms of irreducible spherical tensor operators [18,19]. DQ coherences can be selected using a phase-cycled pulse sequence

$$(\pi/2)_{\varphi} - \tau/2 - (\pi)_{\varphi+90} - \tau/2 - (\pi/2)_{\varphi} - \delta - (\pi/2)_0 - \mathrm{Acq}(t)_{\varphi'},$$

where τ is the double-quantum creation time and δ, the DQ evolution time. The basic four-step phase cycle of the sequence to eliminate SQ coherences is: $\varphi = 0°$, 90°, 180°, 270°; $\varphi' = 2$ (0°, 180°) [12]. In a homogeneous B_1 field and for short δ duration (some μs) this phase cycle yields detectable DQF free induction decay at resonance given by

$$M(t,\tau) = M_0(3/20)[\exp(-\tau/T_{2S}) - \exp(-\tau/T_{2F})] \times [\exp(-t/T^*_{2S}) - \exp(-t/T^*_{2F})], \quad (1)$$

where M_0 is the equilibrium longitudinal magnetization and T^*_{2S} and T^*_{2F} are the B_0-inhomogeneity-broadened forms of T_{2S} and T_{2F} related by

$$1/T^*_{2i} = 1/T_{2i} + \gamma\Delta B_0 \quad (\mathrm{i} = \mathrm{S\ or\ F}), \quad (2)$$

where $\gamma\Delta B_0$ is the inhomogeneity factor.

After Fourier transformation of Eq. (1), the amplitude of the resulting spectrum is

$$S(\omega,\tau) = M_0(3/20)[\exp(-\tau/T_{2S}) - \exp(-\tau/T_{2F})]F(\omega), \quad (3)$$

where $F(\omega)$ is the lineshape function written in terms of the spin–spin relaxation rates R^*_{2S} and R^*_{2F} (equal to $1/T^*_{2S}$ and $1/T^*_{2F}$, respectively) as

$$F(\omega) = R^*_{2S}/(R^{*2}_{2S} + \omega^2) - R^*_{2F}/(R^{*2}_{2F} + \omega^2). \quad (4)$$

To estimate the unknown parameter M_0 from Eq. (3), the relaxation times T_{2S} and T_{2F}, and the B_0 -inhomogeneity (ΔB_0) must be quantified. For the two transverse relaxation times, this is achieved by recording a series of DQ experiments at different τ values and fitting the three-parameter function

$$k \times [\exp(-\tau/T_{2S}) - \exp(-\tau/T_{2F})], \quad (5)$$

to the peak heights (at $\omega = 0$) of the associated DQ spectra [20].

The natural linewidth $1/\pi T^*_2$ measurement with an SQ experiment and the T_2 relaxation time determination with a CPMG sequence allow ΔB_0 to be evaluated using Eq. (2). T^*_{2S} and T^*_{2F} were then calculated, once again using Eq. (2) and previously determined T_{2S} and T_{2F} values.

Finally, the optimum duration of τ (τ^{opt}) that maximizes the amplitude of the DQ signal is determined using the following expression (deduced from Eq. (5))

$$\tau^{\mathrm{opt}} = \frac{\ln(R_{2F}/R_{2S})}{R_{2F} - R_{2S}}. \quad (6)$$

Eqs. (1), (3) and (4) state that DQ filtration places the two relaxing magnetizations in antiphase and that the absorption spectrum is the sum of two lines (L^+ and L^-) of equal areas ($A^{\mathrm{DQ}+} = |A^{\mathrm{DQ}-}|$) but different widths (Fig. 1a), L^+ and L^- widths being related to $1/\pi T^*_{2S}$ and $1/\pi T^*_{2F}$, respectively. To determine the area under the DQ lineshape, an approach roughly similar to that described by Allis et al. [13] was used. It consists in defining the area under the DQ peak as the integral of the lineshape function $F(\omega)$ (Eq. (4)) between the two zero derivative points, defined by $\pm\omega'$, of the function (see Fig. 1b). The area thus determined (see Ref. [13] for details), is given by

$$A^{\mathrm{DQ}} = M_0(3/20)[\exp(-\tau/T_{2S}) - \exp(-\tau/T_{2F})] \times [\tan^{-1}(\omega' T^*_{2S}) - \tan^{-1}(\omega' T^*_{2F})], \quad (7)$$

where

$$\omega' = \left[\left(\sqrt{R^*_{2S}}R^{*2}_{2F} - \sqrt{R^*_{2F}}R^{*2}_{2S}\right)/\left(\sqrt{R^*_{2F}} - \sqrt{R^*_{2S}}\right)\right]^{1/2}. \quad (8)$$

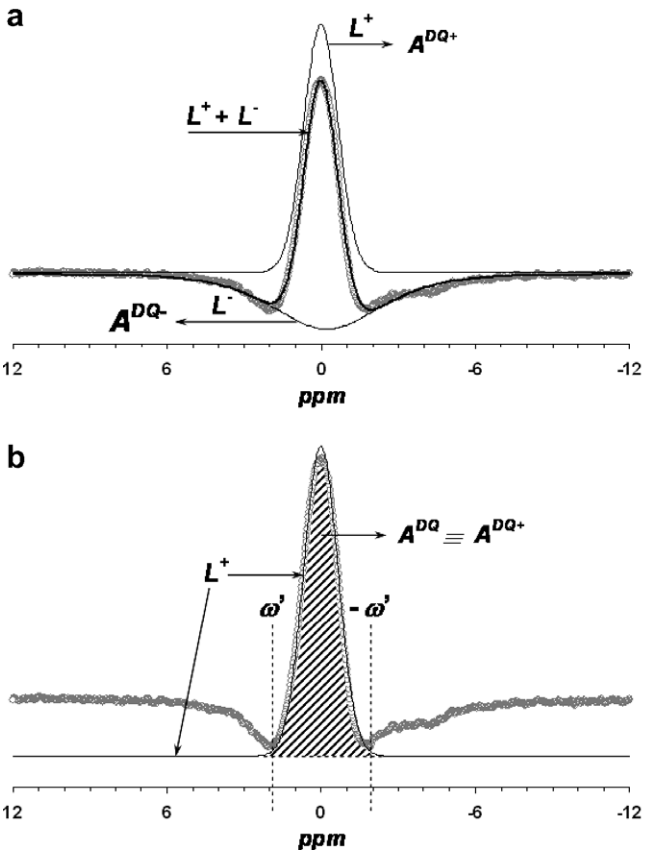

Fig. 1. Experimental (grey circles) DQ spectrum of resin sample ($[Na^+] = 0.71$ M). (a) The lines L^+ and L^- (of area $A^{\mathrm{DQ}+}$ and $A^{\mathrm{DQ}-}$) and their sum (thick line) result from experimental data processing. (b) The lineshape form is given by Eq. (4). and the zero derivative points, $\pm\omega'$, are defined in Eq. (8). The dashed area A^{DQ} is expressed by Eq. (7), and can be estimated by $A^{\mathrm{DQ}+}$ (see text).

Fig. 1b illustrates how A^{DQ} (dashed area) was estimated. The experimental DQ lineshape (grey circle) is the same as that of Fig. 1a, but the L^+ line is presented with a downward translatory to set its baseline tangential to the two zero derivative points at ω' and $-\omega'$. A^{DQ+} is clearly an excellent estimator of A^{DQ}.

To relate M_0 to the concentration of bound Na^+ ions, a calibrated external reference (saline solution) of magnitude M_{REF}, and frequency shifted from the ^{23}Na resonance of the sample, must be used. The area under the SQ reference peak acquired after a $\pi/2$ pulse is obtained by

$$A^{SQ}_{REF} = M_{REF}\pi, \tag{9}$$

This area can be related to the area under the DQ peak (A^{DQ}), combining Eqs. (7) and (9), and M_0 to be calculated

$$M_0 = M_{REF}\frac{10\pi}{3}\frac{A^{DQ}}{A^{SQ}_{REF}}\frac{N^{SQ}}{N^{DQ}}[\exp(-\tau/T_{2S}) - \exp(-\tau/T_{2F})]^{-1} \times [\tan^{-1}(\omega' T^*_{2S}) - \tan^{-1}(\omega' T^*_{2F})]^{-1}, \tag{10}$$

with N^{SQ} and N^{DQ} the number of scans acquired in SQ and DQ experiments, respectively.

3. Experimental

3.1. Sample preparation

A cationic exchange resin (Dowex 50 W × 2, Sigma–Aldrich) was used as model system. Sodium chloride solution (4 M, pH = 5.5) was added to the H^+ form of the resin, of exchange capacity 0.7 M, to replace H^+ by Na^+ ions. The solution was filtered out and the pH of the eluate measured. To ensure complete exchange, mixing and filtering operations were repeated until the pH of the eluate had the same value as the NaCl solution. From this resin sample, three other samples were prepared by mixing it with the H^+ form of the resin in proportions of 25, 50 and 75%, to obtain theoretical Na^+ ion concentrations of 0.52, 0.35 and 0.17 M, respectively. A calibrated (0.5 M) aqueous solution of $Na_7Dy(PPP)_2$ was prepared and used as external reference to check (i) the sodium ion content of the four samples, the $Dy(PPP)_2^{7-}$ ion inducing an upfield shift of Na^+ (≈ 17 ppm) from the resin resonance position, and (ii) the efficiency of the DQF pulse sequence in suppressing the Na^+ signal associated with the free ions. The composite phantom thus prepared consists of two coaxial tubes of 10 mm (external: containing resin) and 5 mm (internal: containing reference). The volume ratio V_{RESIN}/V_{REF} of 3.26 was obviously taken into account for the Na^+ quantification.

After these preliminary experiments, SQ and DQ spectra were recorded on resin samples without inserting an external reference, the resin becoming its own reference ($M_0 = M_{REF}$ in Eq. (10)), all Na^+ ions contained in the resin samples being in a bound state.

3.2. NMR experiments and data processing

All NMR experiments were performed at 106 MHz (^{23}Na) on a Bruker DRX-400 (9.4 T) instrument using a 10 mm double-tuned $^1H/^{23}Na$ NMR probe built in-house. Samples were maintained in the spectrometer at 25 °C. The on-resonance $\pi/2$ pulse length was 17 μs. Na^+ relaxation times T_1 and T_2 of the four resin samples were determined from inversion-recovery (16 inter-pulse delays from 1 to 500 ms) and CPMG (64 echo times from 2 to 128 ms) experiments.

Double-quantum filtered NMR spectra were acquired for 16 τ values, ranging between 200 μs and 60 ms, to determine T_{2S}, T_{2F} and calculate τ^{opt} values. SQ ($\pi/2$ pulse) and DQ (using τ^{opt}) acquisitions were then recorded on the four samples with identical numbers of scans (128), repetition times (250 ms) and receiver gains.

SQ and DQ spectra were analyzed with PeakFit software. Gaussian–Lorentzian sum was used as the lineshape function for the lineshape adjustment.

4. Results and discussion

4.1. Sample characterization

Na^+ concentrations of the four resin samples ($[Na]^{SQ}$) were estimated as described in the experimental part, from the comparison between the area of resin and external reference SQ signals (A^{SQ} and A^{SQ}_{REF}) as follows:

$$[Na]^{SQ} = \frac{A^{SQ}}{A^{SQ}_{REF}} \times \frac{[Na]^{SQ}_{REF}}{3.26}. \tag{11}$$

The values thus determined (0.71, 0.54, 0.33 and 0.16 M) were in close agreement with those expected (0.70, 0.52, 0.35 and 0.17 M). This also indicates that all Na^+ ions contained in the resin, despite being in a bound state, were detected.

The SQ and DQ Na^+ signals of the resin (0.71 M) containing the external reference (0.5 M) are shown in Fig. 2. Two remarks can be made: (i) the DQ signal intensity of the resin is very weak compared with the SQ signal intensity (factor of 40 between the two spectra), and (ii) there is a very small residual signal from the reference in the DQ spectra. The first remark will be discussed in the quantification section. The second is explained by the off-resonance position of the reference peak, which lowers the efficiency of the DQ filter.

In our experimental conditions, T_1 and T_2 relaxation curves were closely fitted to mono-exponential functions. Their values were found to be similar for the four samples: 24.4 ± 0.1 and 18.5 ± 0.1 ms, respectively.

Fig. 3 presents the variation of the DQ peak intensity (I^{DQ}) as a function of the DQ creation time τ for the resin at 0.71 M. A similar evolution was obtained for the four samples studied and the mean τ^{opt} value of 4.8 ± 0.1 ms,

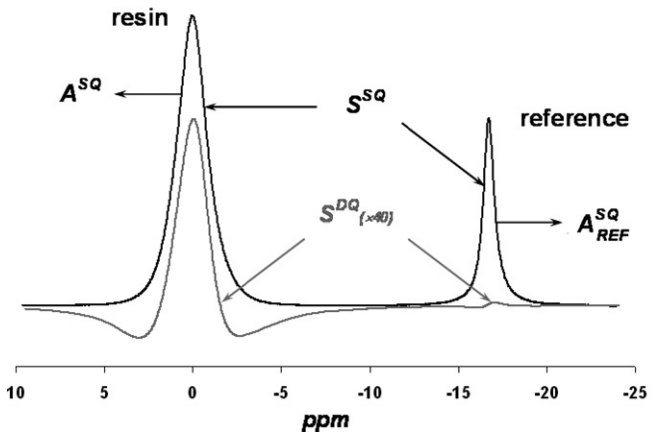

Fig. 2. SQ (black line) and DQ (grey line) spectra of resin ($[Na^+] = 0.71$ M) with the inserted reference ($[NaCl] = 0.5$ M). Note that the DQ spectrum is magnified by a factor of 40.

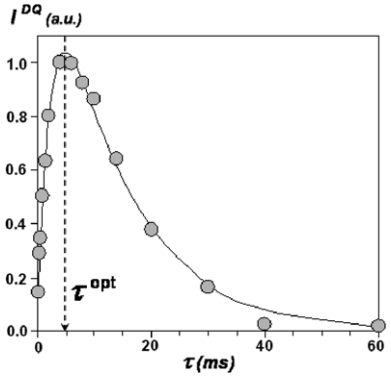

Fig. 3. DQ peak intensity evolution of resin sample ($[Na^+] = 0.71$ M) *vs.* the creation time τ. Solid line is the curve obtained by fitting Eq. (5).

deduced from the fitting procedure (Eq. (5)) and using Eq. (6), was then used to obtain the maximum DQ signal.

4.2. Absolute quantification

After SQ and DQ spectra adjustment, two ratio mean values (homogeneity of results for the four samples studied) were calculated: $A^{DQ+}/|A^{DQ-}| = 1.03 \pm 0.02$ and $(A^{DQ+} + |A^{DQ-}|)/A^{SQ} = 0.022 \pm 0.001$. The first ratio validates the data processing by corroborating that the DQ filter leads to a lineshape that is the sum of two lines in antiphase with equal area (Fig. 1a). The second states that experimentally, the total DQ area represents only 2.2% of the SQ area ($[Na]^{DQ}_{EXP} = 0.022 \times [Na]^{SQ}$). This demonstrates that it is not possible to quantify the Na^+ bound fraction, which is 100% for the present model system, directly from a basic analysis of the experimental peak areas.

In our experimental conditions, Eq. (10) can be rewritten as

$$[Na]^{DQ}_{CALC} = [Na]^{SQ} \frac{10\pi}{3} \frac{A^{DQ+}}{A^{SQ}} [\exp(-\tau/T_{2S}) - \exp(-\tau/T_{2F})]^{-1} \times [\tan^{-1}(\omega' T^*_{2S}) - \tan^{-1}(\omega' T^*_{2F})]^{-1}, \quad (12)$$

SQ and DQ parameters necessary for the quantification procedure are summarized in Table 1. Substituting T^*_{2S} and T^*_{2F} into Eq. (8) gave $\omega' = 1254 \pm 25$ rad s^{-1}, corresponding to a frequency width $2\omega'/2\pi$ of 400 Hz, which agreed perfectly with experimental spectra (see Fig. 1b). Finally, substituting all these parameters by their values in Eq. (12), the Na^+ concentrations calculated ($[Na]^{DQ}_{CALC}$) for the four resin samples are: 0.69, 0.53, 0.34 and 0.15 M. These results are presented in Fig. 4, which also shows concentrations determined from the DQ lineshape area analysis ($[Na]^{DQ}_{EXP}$). The associated linear regressions are: $[Na]^{DQ}_{CALC} = 0.98 * [Na]^{SQ} (R^2 = 0.997)$ and $[Na]^{DQ}_{EXP} = 0.022 * [Na]^{SQ} (R^2 = 0.995)$. Thus although the residual DQ signal is only 2.2% of the SQ signal, instead of the 100% expected, the quantification procedure developed allows us to obtain the true concentrations of Na^+ bound ions in the resin system used ($[Na]^{DQ}_{CALC} \cong [Na]^{SQ}$).

With all sodium ions bound to the resin, there are equal populations contributing to the SQ and DQ signals. The equality of SQ and DQ signals makes it possible to validate the sodium concentration quantifications (see Fig. 4, black circles). Table 1 highlights a significant difference between T_2 and T_{2S}, even though it is generally accepted that they are equal in the case of no contribution of second rank ten-

Table 1
Relaxation times, inhomogeneity factor ($\gamma\Delta B_0$), optimal double-quantum creation time (τ^{opt}) and zero derivative point (ω') of the lineshape function $F(\omega)$ for Na^+ in resin

SQ experiments	DQ experiments	SQ–DQ combination
$T_2 = 18.5 \pm 0.1$ ms	$T_{2S} = 12.7 \pm 0.2$ ms	$T^*_{2S} = 1.78 \pm 0.03$ ms
$T^*_2 = 1.87 \pm 0.08$ ms	$T_{2F} = 2.3 \pm 0.1$ ms	$T^*_{2F} = 1.09 \pm 0.01$ ms
(↓Eq. (2))	(↓Eq. (6))	(↓Eq. (8))
$\gamma\Delta B_0 = 480 \pm 30$ s^{-1}	$\tau^{opt} = 4.8 \pm 0.1$ ms	$\omega' = 1254 \pm 25$ rad s^{-1}

The standard deviations (±) indicated were calculated from ($n = 4$) different resins.

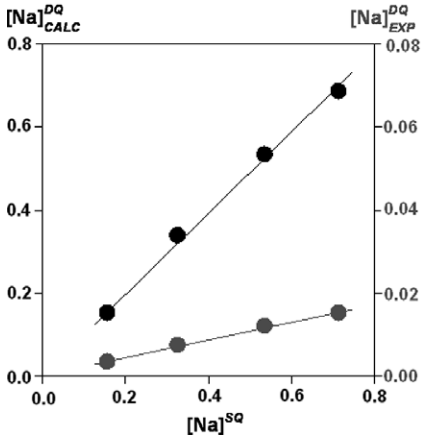

Fig. 4. Sodium concentrations calculated with Eq. (12) ($[Na]^{DQ}_{CALC}$; black circles) and estimated from the DQ lineshape area ($[Na]^{DQ}_{EXP}$; grey circles) *vs.* those obtained from SQ spectra analysis, for the four resin samples studied. Straight lines result from linear regressions (see text for details).

sor ($\mathbf{T}_{2,2}$) to the DQ transverse relaxation [17]. The observed difference can be explained by this tensor's contribution [21], which is consistent with the lower T_{2S} value compared to T_2.

Finally, we can note that the efficiency of DQ signal generation depends not only on the ratio T_{2S}/T_{2F} [22,23] but also on $\gamma\Delta B_0$ *via* the ratio T^*_{2S}/T^*_{2F}, a decrease in one (or both) of these ratios inducing a decrease in the DQ signal amplitude. In the case of our model system, the relatively high value of $\gamma\Delta B_0$, probably due to an internal magnetic susceptibility effect (presence of small air bubbles), explains why the residual DQ signal is only 2.2% of the SQ signal.

5. Conclusions

We have shown how signals from bound sodium ions can be precisely quantified by double-quantum filtration. The analytical approach presented needs the accurate determination of T_{2S}, T_{2F} and ΔB_0. This method can be applied to a large set of systems for which sodium ions interact strongly with their environment and need to be quantified. Work on the use of this approach is currently in progress for the study of processed food products, e.g., smoked salmon fillets, hams and cheeses. The aim is to reduce the quantity of salt added without adversely affecting either the shelf life of the product or consumer satisfaction in terms of taste. For this purpose, there is a need to characterize and quantify the content and evolution of salt (NaCl) in these products subject to salting/brining/drying processes. This can be done through the SQ and DQ detection of sodium nuclei. In addition, the precise quantification of Na^+ bound and free fractions is of particular interest as regards their relative contributions to the salt taste.

References

[1] P. Porion, M. Al Mukhtar, S. Meyer, A.M. Faugere, J.R.C. van Maarel, A. Delville, Nematic ordering of suspensions of charged anisotropic colloids detected by ^{23}Na nuclear magnetic resonance, J. Phys. Chem. B 105 (2001) 10505–10514.

[2] L.A. Rijniers, P.C.M.M. Magusin, H.P. Huinink, L. Pel, K. Kopinga, Sodium NMR relaxation in porous materials, J. Magn. Reson. 167 (2004) 25–30.

[3] D.E. Woessner, NMR relaxation of spin-3/2 nuclei: Effects of structure, order, and dynamics in aqueous heterogeneous systems, Concepts Magn. Reson. 13 (2001) 294–325.

[4] U. Eliav, G. Navon, Analysis of double-quantum-filtered NMR spectra of ^{23}Na in biological tissues, J. Magn. Reson. B 103 (1994) 19–29.

[5] R. Reddy, L. Bolinger, M. Shinnar, E. Noyszewski, J.S. Leigh, Detection of residual quadrupolar interaction in human skeletal muscle and brain in vivo via multiple quantum filtered sodium NMR spectra, Magn. Reson. Med. 33 (1995) 134–139.

[6] S. Olt, E. Krötz, E. Komor, M. Rokitta, A. Haase, ^{23}Na and 1H NMR microimaging of intact plants, J. Magn. Reson. 144 (2000) 297–304.

[7] L. Foucat, J.P. Donnat, J.P. Renou, ^{23}Na and ^{35}Cl NMR studies of the interactions of sodium and chloride ions with meat products, in: P.S; Belton, A.M. Gil, G.A. Webb, D. Rutledge (Eds.), Magnetic Resonance in Food Science; Latest Developments, Cambridge, 2003, pp. 180–185.

[8] L. Foucat, R. Ofstad, J.P. Renou, How is the fish meat affected by technological processes?, in: G.A. Webb (Ed.), Modern Magnetic Resonance, New York, 2006, pp. 957–961.

[9] C. Vestergaard, J. Risum, J. Adler-Nissen, ^{23}Na-MRI quantification of sodium and water mobility in pork during brine curing, Meat Sci. 69 (2005) 663–672.

[10] U. Erikson, E. Veliyulin, T.E. Singstad, M. Aursand, Salting and desalting of fresh and frozen-thawed cod (*Gadus morhua*) fillets; a comparative study using Na-23 MRI, low-field H-1 NMR, and physicochemical analytical methods, J. Food Sci. 69 (2004) E107–E114.

[11] M. Ruusunen, E. Puolanne, Reducing sodium intake from meat products, Meat Sci. 70 (2005) 531–541.

[12] R. Kemp-Harper, S.P. Brown, C.E. Hughes, P. Styles, S. Wimperis, ^{23}Na NMR methods for selective observation of sodium ions in ordered environments, Prog. Nucl. Magn. Res. Spect. 30 (1997) 157–181.

[13] J.L. Allis, A.-M.L. Seymour, G.K. Radda, Absolute quantification of intracellular Na^+ using triple-quantum-filtered sodium-23 NMR, J. Magn. Reson. 93 (1991) 71–76.

[14] J. Whang, J. Katz, L.M. Boxt, K. Reagan, D.J. Sorce, R.R. Sciacca, P.J. Cannon, Multiple-quantum-filtered NMR determination of equilibrium magnetization for ^{23}Na quantitation in model phantoms, J. Magn. Reson. 103 (1994) 175–179.

[15] K.J. Jung, P.J. Cannon, J. Katz, Measurement of transverse relaxation times and content ratio of ^{23}Na in phantoms simulating biological systems by use of multiple-quantum filtering, J. Magn. Reson. 124 (1997) 393–399.

[16] P.S. Hubbard, Nonexponential nuclear magnetic relaxation by quadrupole interactions, J. Chem. Phys. 53 (1970) 985–987.

[17] G. Jaccard, S. Wimperis, G. Bodenhausen, Multiple-quantum NMR spectroscopy of $S = 3/2$ spins in isotropic phase: A new probe for multiexponential relaxation, J. Chem. Phys. 85 (1986) 6282–6293.

[18] N. Müller, G. Bodenhausen, R.R. Ernst, Relaxation-induced violations of coherence transfer selection rules in nuclear magnetic resonance, J. Magn. Reson. 75 (1987) 297–334.

[19] J.R.C. van der Maarel, Thermal relaxation and coherence dynamics of spin 3/2. I. Static and fluctuating quadrupolar interactions in the multipole basis, Concept Magn. Reson. 19A (2003) 97–116.

[20] J. Pekar, J.S. Leigh Jr., Detection of biexponential relaxation in sodium-23 facilitated by double-quantum filtering, J. Magn. Reson. 69 (1986) 582–584.

[21] H. Shinar, T. Knubovetz, U. Eliav, G. Navon, Sodium interaction with ordered structures in mammalian red blood cells detected by Na-23 double quantum NMR, Biophys. J. 64 (1993) 1273–1279.

[22] W.D. Rooney, T.M. Barbara, C.S. Springer Jr., Two-dimensional double-quantum NMR spectroscopy of isolated spin 3/2 systems: ^{23}Na examples, J. Am. Chem. Soc. 110 (1988) 674–681.

[23] L.A. Jelicks, R.K. Gupta, Observation of intracellular sodium ions by double-quantum-filtered ^{23}Na NMR with paramagnetic quenching of extracellukar coherence by gadolinium tripolyphosphate, J. Magn. Reson. 83 (1989) 146–151.